

Design and Development of a Neural Surface Rendering Model for Lunar Satellite Photogrammetry

Caleb Adams, Ignacio Lopez-Francos, Ariel Deutsch, Ellemieke Van Kints, Aiden Hammond

Intelligent Systems Division
 NASA Ames Research Center
 Moffet Field, CA, USA
 caleb.a.adams@nasa.gov

ABSTRACT

Neural volumetric scene representations encode the color and density of points in 3D space by optimizing an underlying continuous volumetric scene function. These methods are focused on synthesizing novel views of objects and on-ground scenes from a set of sparse input views. However, they under-perform at photogrammetric tasks of geometric reconstruction from multi-view satellite imagery in environments with diffuse reflection and harsh shading. This limits the ability of these methods to accurately generate Digital Elevation Models (DEMs) of the permanently shadowed regions (PSRs) on the lunar surface, which are critical targets for NASA's Artemis mission. Therefore, the goal of this research is to cherry-pick geometric and physics-based features from recent neural scene representation methods and present a theoretical surface rendering model for reconstructing the lunar surface. Specifically, we are interested in generating DEMs of the lunar surface and relighting its permanently shadowed regions (PSRs) using multi-view satellite imagery. By incorporating techniques such as a learned distance function of the surface geometry and an explicit illumination model, we aim to present a new neural rendering scheme for surface reconstruction tailored specifically to the lunar environment.

INTRODUCTION

Satellite-based stereophotogrammetry (SP) offers a passive method for monitoring the lunar surface. SP methods transform 2D images into 3D visual models, which can provide a more comprehensive representation of a particular target compared to the 2D images alone. The resulting 3D models can be used for quantifying landscape parameters, such as relief or surface texture.^{1,2} Traditional SP methods perform 3D reconstruction by identifying and matching feature points across multiple images.³ However, these feature points are difficult to detect in areas with complicated lighting conditions and homogeneous physical characteristics, resulting in sparse and discontinuous reconstructions. The permanently shadowed regions (PSRs) on the Moon, which are critical targets for NASA's Artemis mission, exhibit harsh shading and diffuse reflection. Thus, traditional SP methods often struggle to create accurate 3D models of the terrain. Today, critical algorithmic gaps exist in traditional SP methods that hinder their use for observing lunar PSRs.

Neural Radiance Fields (NeRFs) might address these limitations by employing a multi-layer perceptron (MLP) network to learn the optimal features for an

individual 3D scene.⁴ NeRFs break away from traditional photogrammetric assumptions of rigid surfaces, and instead, use reverse rendering techniques to predict the radiance and density of a point in 3D space. This allows for a more comprehensive representation of the reconstructed scene, in terms of both color and geometry. Once a NeRF is trained to completion, novel views of the scene can be rendered and 3D data products can be extracted.

NeRF methods for satellite-based SP have recently emerged, namely Shadow-NeRF (S-NeRF),⁵ Satellite-NeRF (Sat-NeRF),⁶ and Earth Observation NeRF (EO-NeRF).⁷ These methods propose a number of improvements to the original NeRF, including an explicit light transport model that simultaneously takes into account occlusion and varying illumination effects and a novel point sampling strategy attuned to the characteristics of satellite imagery.⁵ As a result, the color and geometry of the 3D scene is improved, particularly in shadowed areas that lack distinctive visual features. Our initial work into these methods revealed that they succeed at reconstructing simulated lunar environments and generating shadow-free renderings of the terrain.

Advances have also been made towards representing surfaces as the zero-level set of a neural implicit distance function^{8,9}. These functions are designed to predict distances from a point in space to the nearest surface. We focused on two variants of distance functions, Neural Implicit Surfaces (NeuS)⁸ and Neural Unsigned Distance Functions (NeUDF)⁹, which employ Signed Distance Functions (SDFs) and Unsigned Distance Functions (UDFs) respectively. While UDFs only represent the magnitude of the distance, SDFs include sign information, denoting whether a point is within or outside of a surface. These distance functions offer robustness against sudden depth changes over density-based scene representations and are able to be used in combination with volume rendering techniques^{8,9}.

In this paper, we introduce our ideas for a theoretical neural scene representation method for lunar surface reconstruction and relighting from diverse datasets, which we call Lunar Neural Radiance Methods (LunarNRM), and show our initial results for the currently supported methods. LunarNRM will encode geometric and physical scene properties through the use of NeRF MLP networks. Heterogeneous lunar-observation data products, such as Lunar Reconnaissance Orbiter Camera (LROC) pushbroom image scans and Lunar Orbiter Laser Altimeter (LOLA) Digital Elevation Models (DEMs), will be used as input to our method and fused with other sensor measurements to guide the learning process and enforce physical correctness. Incorporating diverse lunar-observation data products from NASA sensors in a novel NeRF pipeline will allow us to fill in the gaps of traditional SP methods and produce physically accurate DEMs of lunar PSRs.

We have so far explored both density-based and SDF-based approaches for lunar surface modeling using simulated lunar imagery. LunarNRM currently supports the standard density-based NeRF model with ReLU activations and a variation of the Gaussian Activated Radiance Fields (GARF) model, which we call GaussNeRF.¹⁰ The SDF-based methods currently supported are NeuS and NeuDF.^{8,9} Additionally, both basic and Gaussian Random Fourier Feature encoding are supported. The experiments presented in this paper are outlined in *Table 1*. We test each method in LunarNRM with four simulated lunar datasets compiled from Blender. The small-scale lunar scene covers $5 \times 5 \times 0.75$ meters, and the large-scale lunar scene covers $700 \times 700 \times 67.4$ meters. Sample images from each scene can be seen in *Figure 1* and *3*, and their ground-truth point clouds can be seen in *Figure 2* and *4*. Camera poses were

estimated using COLMAP and directly extracted from Blender using the Blender Photogrammetry Importer^{11,12,13}.

Table 1: Outline of LunarNRM experiments presented in this paper.

Experiment Number	Model Type	Scene Scale	Camera Poses
1	NeRF, Pos. Enc.	Small-Scale	COLMAP
2	NeRF, Pos. Enc.	Small-Scale	True Poses
3	NeRF, Pos. Enc.	Large-Scale	COLMAP
4	NeRF, Pos. Enc.	Large-Scale	True Poses
5	NeRF, Gauss. RFF	Small-Scale	COLMAP
6	NeRF, Gauss. RFF	Small-Scale	True Poses
7	NeRF, Gauss. RFF	Large-Scale	COLMAP
8	NeRF, Gauss. RFF	Large-Scale	True Poses
9	GaussNeRF	Small-Scale	COLMAP
10	GaussNeRF	Small-Scale	True Poses
11	GaussNeRF	Large-Scale	COLMAP
12	GaussNeRF	Large-Scale	True Poses
13	NeuS	Small-Scale	COLMAP
14	NeuS	Small-Scale	True Poses
15	NeuDF	Small-Scale	COLMAP
16	NeuDF	Small-Scale	True Poses

The performance of each model in LunarNRM is quantitatively evaluated using two separate metrics:

1. Mean Peak Signal to Noise Ratio (PSNR) of novel views
2. Mean Signed Distance between the predicted and ground-truth point clouds

Our initial results show that the basic density-based NeRF model with Gaussian activations achieves the highest accuracy at both tasks of novel view synthesis and surface reconstruction using large-scale simulated lunar data, as indicated by the highest mean PSNR score on test data and lowest mean signed distance between the generated and ground-truth point clouds. Additionally, the NeRF model with ReLU activations and a basic positional embedding layer achieved the highest accuracy for the small-scale simulated lunar data. Our proposed method also incorporates a re-scale step, making it generalizable to both large-scale and small-scale lunar environments. Overall, in this



Figure 1: Reference image from the small-scale simulated lunar scene ($5 \times 5 \times 0.75$ meters).



Figure 3: Reference image from the large-scale simulated lunar scene ($700 \times 700 \times 67.4$ meters).



Figure 2: Ground-truth point cloud of the small-scale simulated lunar scene ($5 \times 5 \times 0.75$ meters).

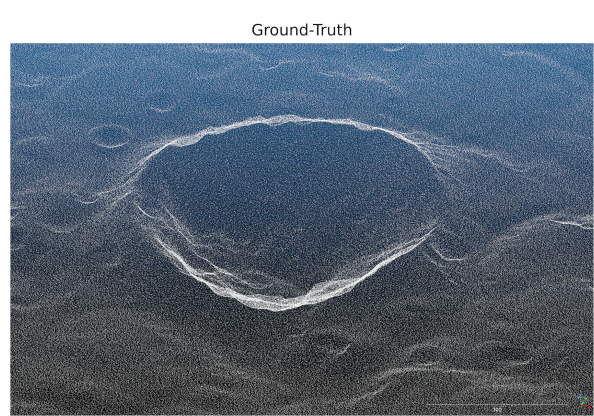


Figure 4: Ground-truth point cloud of the large-scale simulated lunar scene ($700 \times 700 \times 67.4$ meters).

paper we show that our method can successfully reconstruct simulated lunar craters of various scales with high visual and geometric accuracy. Lastly, we discuss our theoretical framework for expanding LunarNRM to produce physically accurate shadow-free renderings from heterogeneous datasets in our Future Works section.

RELATED WORK

Nerfacto

Our prior work explored Nerfacto from the NeRFStudio framework. We used this as our baseline method because it is highly generalized and thus an adequate starting point. NeRFacto is a combination of many published methods¹⁴ and offers the same capabilities as a typical NeRF; notably it does not offer shadow removal nor relighting capability. NeRFStudio provides a COLMAP method of processing a set of images into a dataset that is usable within the framework. This method produces qualitatively accurate results for novel view synthesis.¹⁵ Recently, NeRFStudio implemented Gaussian Splatting.¹⁶ This produces visually appealing results but it non-viable for our MLP-based relighting strategies.

NeRF for Satellite Photogrammetry

A primary method of interest is Shadow NeRF (S-NeRF), a shadow-aware method for multi-view satellite photogrammetry. S-NeRF extends the traditional NeRF method by introducing an explicit shading model and enables shadow-free rendering of a scene. Compared to traditional methods,¹⁷ S-NeRF provides more accurate shape and color synthesis in shaded areas.⁵

To model variations in incoming light, S-NeRF introduces two new physical properties, the ratio of incoming solar light and the sky color. These values are learned by the neural network and are used to calculate the intensity of incoming light, or irradiance, at a 3D location. Unlike the original NeRF implementation, S-NeRF generates albedo as a network output.^{5,17} The learned albedo and irradiance values are used to calculate the radiance for a given point in 3D space. This allows S-NeRF to remove shadows from the rendered scene and estimate color from areas that are permanently in the shadows in the training images.⁵

To determine its abilities at reconstructing lunar environments, we tested S-NeRF using a simulated orbital lunar dataset with varying lighting conditions.

Our initial results can be seen in *Figure 5*. S-NeRF achieved mean PSNR/SSIM scores of 21.2/0.48 on test data and an altitude mean average error (MAE) of 33.24 meters. These results indicate that S-NeRF can successfully render novel views of lunar environments from simulated orbital data. However, the altitude MAE is three times higher than what is reported with the real-world urban datasets in the S-NeRF paper. This difference highlights the unique challenges posed by lunar terrain reconstruction, such as surface homogeneity, which is less pronounced in urban settings which have defined edges from buildings and variations in color and surface texture. This necessitates further refinement of S-NeRF to improve its geometric accuracy in extraterrestrial applications. Future work will focus on fusing heterogeneous lunar-observation products to aid the MLP network in accurately reconstructing the scene geometry and estimating the surface altitude.

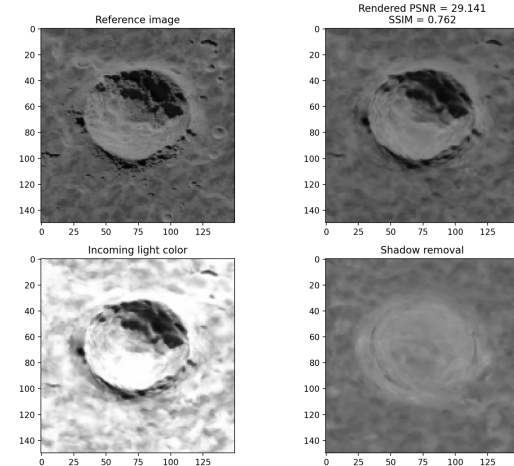


Figure 5: S-NeRF reference image (top-left), rendered image (top-right), calculated incoming light (bottom-left), and rendered image with removed shadows (bottom-right).

Satellite NeRF, or Sat-NeRF, incorporates well-known techniques for satellite images processing into a NeRF framework.⁶ In particular, Sat-NeRF represents each input image as an RPC model, characteristic of satellite images, instead of a pinhole camera model commonly used in NeRF for close-range imagery. RPC models consist of a set of polynomial functions that can translate between 2D pixel space and 3D scene space via projection and localization functions. Sat-NeRF directly uses these RPC models to cast rays into the scene space.

Sat-NeRF further refines the the RPC model for each image by means of bundle adjustment, which

minimizes the reprojection error of points in the 3D scene. Bundle adjustment is commonly done in SP to correct RPC inconsistencies. Before training a Sat-NeRF model, bundle adjustment can be applied to correct the RPC models of all input images. The authors of Sat-NeRF found that the use of bundle adjusted RPC models directly increased the accuracy of the point sample strategy.⁶ The combination of these factors enables Sat-NeRF to render new views and infer surface models of similar quality to those obtained with traditional state-of-the-art stereo pipelines.

As an extension to both S-NeRF and Sat-NeRF, EO-NeRF develops a geometrically consistent shadow model. However, it is important to note that the code for EO-NeRF has not yet been published. EO-NeRF highlights the use of multi-date NeRFs for rendering volume rendering which does *not* predict shadows, but renders them according to the geometry and position of the Sun.⁷ In addition, EO-NeRF uses Universal Transverse Mercator (UTM) coordinates and network parameters to address inaccuracies in the camera models, in addition to other strategies, to process raw satellite imagery in contrast to pre-processed imagery. These extensions allow EO-NeRF to output a variety of information, including geometric shadows, uncertainty, transience, and albedo with/without irradiance from geometric shadows while outperforming S-NeRF, Sat-NeRF, and state-of-the-art stereo-vision methods.⁷

GARF

Gaussian Activated neural Radiance Fields (GARF) employ Gaussian activations instead of ReLU activations.¹⁰ In traditional NeRF methods, the low-dimensional input coordinates are projected to a higher dimension via a positional embedding layer. The embedded 3D input points are then passed through a conventional ReLU MLP. This allows the MLP to learn higher frequency functions and thus capture the finer details in a scene. However, MLPs which use ReLU activation and positional embeddings are incapable of accurately modeling first-order derivatives of the target signal, resulting in noisy artifacts.¹⁰ Gaussian activations, on the other hand, preserve the first-order gradients of the target function, leading to more accurate results in terms of high-fidelity reconstruction.

When trying to represent a low-dimensional signal as an implicit neural function, ReLU networks fail. No matter how many sample points are used, or how deep the network is, there is an indicative bias that

smooths the signal out.¹⁰ To circumvent this issue, NeRF architecturally modifies the MLPs with a positional embedding layer. This adds bandwidth to the network and counteracts the bias introduced by ReLU activations. However, ReLU networks with positional embeddings can lead to noisy gradients. The GARF paper empirically shows that the ability of the model to preserve the first-order gradients of the target function plays an imperative role in radiance field reconstruction.¹⁰ Thus, activations that better maintain the fidelity of these first-order gradients can be used to directly improve the accuracy of the reconstructed signal.

By using Gaussian activations instead of ReLU activations, GARF is able to increase the bandwidth of low-dimensional signals without the need for a positional embedding layer. Unlike sinusoid activations, which are sensitive to initialization, Gaussian activations work well with standard model initializations, making them more robust and easier to implement. This advancement not only simplifies the architecture but also enhances the quality of the rendered scenes by reducing artifacts and preserving the fine details, thereby setting a new standard for neural radiance field reconstructions.

Neural Distance Functions

We are exploring NeuS and NeUDF as Neural Distance Function solutions. NeuS employs a neural network to represent both the geometry and appearance of a scene, which maps a 3D position to its signed distance to the nearest surface and encodes the color information. The surface of the object is defined as the zero-level set of the SDF. The network is trained using a novel volume rendering approach that ensures robust optimization and accurate surface reconstruction.⁸

An innovation in NeuS is the introduction of an S-density field, which is derived from the logistic density distribution. This field allows volume rendering to be applied to the SDF, providing a probabilistic framework that makes the optimization process robust against the sparsity and noise of the input data.⁸

NeUDF employs a neural network to predict the unsigned distance field while simultaneously optimizing the rendering process. This is achieved through differentiable rendering. The UDF is used to calculate the intensity of light at various points, enabling the network to accurately reconstruct the 3D geometry.⁹

LUNARNRM

NeRF with PE

NeRF was introduced with a Fourier feature encoding scheme,⁴ meant to let the networks learn high frequency functions in low dimensional domains.¹⁸ This scheme is described by γ in Equation 1 where p is an arbitrary input in \mathbb{R} and L is a manually set positive integer.

$$\gamma(\mathbf{p}) = [\cos(2^0\pi\mathbf{p}), \sin(2^0\pi\mathbf{p}), \dots, \cos(2^{L-1}\pi\mathbf{p}), \sin(2^{L-1}\pi\mathbf{p})] \quad (1)$$

γ maps from \mathbb{R} to a higher dimensional space \mathbb{R}^{2L} to enable the MLP to learn higher frequency functions.⁴ Our initial novel view synthesis results with this method of positional encoding are shown in *Figure 6* and *Figure 7*, for the small-scale and large-scale lunar datasets with estimated camera poses, respectively. We observe that both novel view synthesis and surface reconstruction improve with the use of accurate camera poses from the simulated Blender scene. Our results using accurate camera poses can be seen in *Figure 13* and *14*.

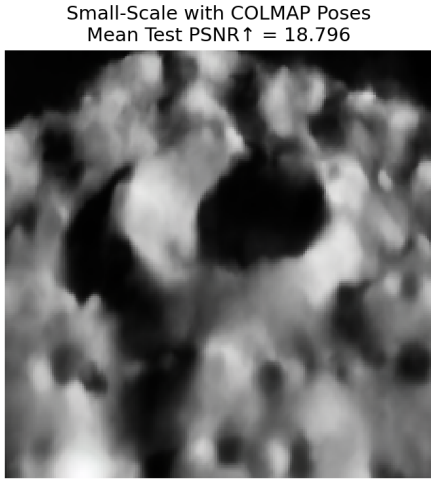


Figure 6: Novel view synthesis results for Experiment 1. NeRF with basic PE was tested with the small-scale lunar dataset with estimated camera poses from COLMAP.

Our results suggest that the basic positional encoding method can succeed in reconstructing the surface and rendering novel views for the small-scale lunar scene. We see less accuracy overall for large-scale lunar scenes, indicating that NeRF with basic positional encoding achieves better results with smaller lunar scenes. The use of accurate camera

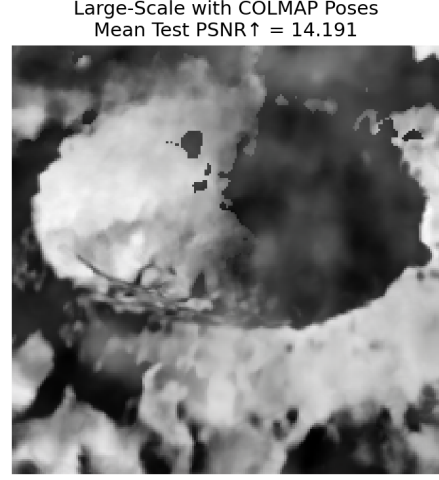


Figure 7: Novel view synthesis results for Experiment 3. NeRF with basic PE was tested with the large-scale lunar dataset with estimated camera poses from COLMAP.

poses from the simulated Blender scene improved our results for both scene sizes. When using camera poses estimated with COLMAP, we observe less accurate reconstructions and novel view syntheses. This discrepancy highlights the importance of precise camera pose estimation in achieving high-quality results. Additionally, the network overestimated the surface altitude in the shadowed areas of the craters, thus performing poorly in comparison to non-shadowed areas, which was expected.

NeRF with Gaussian RFF PE

Gaussian Random Fourier Feature (RFF) mapping is regarded as the best positional embedding method for 3D inverse rendering for view synthesis.¹⁸ The equation is described as

$$\gamma(v) = [\cos(2\pi\mathbf{Bv}), \sin(2\pi\mathbf{Bv})]^T \quad (2)$$

where each entry in $\mathbf{B} \in \mathbb{R}^{m \times d}$ is sampled from $\mathcal{N}(0, \sigma^2)$, and σ is chosen for each task and dataset through hyperparameter tuning. The σ serves the same purpose as the number of levels in positional encoding. In our experiments, we set σ to 6 by default.

Our initial novel view synthesis results for both the large-scale and small-scale simulated lunar environments with estimated camera poses are presented in *Figure 8* and *9*. As with basic positional encoding, we observe that Gaussian RFF encoding achieves

more accurate results for small-scale lunar scenes, compared to large-scale lunar scenes. Additionally, we observe that both novel view synthesis and surface reconstruction for both scenes improve with the use of accurate camera poses. Our results using accurate camera poses can be seen in *Figure 13* and *14*.

Interestingly, the NeRF method with basic positional encoding outperformed the NeRF method with Gaussian RFF in both tasks for the scaled-down simulated lunar dataset. This contrasts with previous research that highlighted the advantages of Gaussian RFF encoding for view synthesis.¹⁸ However, for the scaled-up simulated lunar dataset, Gaussian RFF achieved more accurate results than basic positional encoding for both novel view synthesis and surface reconstruction. Overall, our initial results suggest that basic positional encoding produces more accurate results for small-scale lunar scenes only, while Gaussian RFF encoding shows superior performance for larger-scale scenes, indicating a scale-dependent effectiveness. Future work will focus on investigating the underlying factors that contribute to the varying performance of each encoding method.

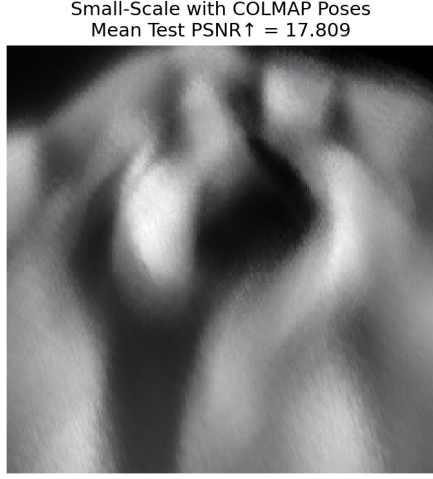


Figure 8: Novel view synthesis results for Experiment 5. NeRF with Gaussian RFF PE was tested with the small-scale lunar dataset with estimated cameras poses from COLMAP.

GaussNeRF

The GaussNeRF model in LunarNRM is based off GARN.¹⁰ GaussNeRF contains the same architecture as the basic NeRF model, but no positional embedding layer is used and Gaussian activations are used instead of ReLU. Our initial results in *Figure*

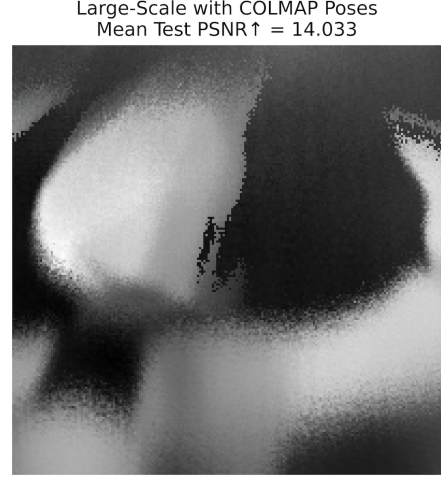


Figure 9: Novel view synthesis results for Experiment 7. NeRF with Gaussian RFF PE was tested with the large-scale lunar dataset with estimated camera poses from COLMAP.

14 show that these small changes improve results for both tasks of novel view synthesis and surface reconstruction for the large-scale simulated lunar dataset. Our initial novel view synthesis results for both the large-scale and small-scale simulated lunar scenes with estimated camera poses are presented in *Figure 10* and *11*. When using estimated camera poses, GaussNeRF achieves more accurate results at novel view synthesis for the small-scale lunar scene. However, when using accurate camera poses, GaussNeRF achieves more accurate results for the large-scale lunar scene.

Compared to the basic NeRF model with Gaussian RFF positional encoding, the GaussNeRF model produced more accurate results with the large-scale simulated lunar dataset, as indicated by higher mean PSNR scores on test data and lower mean signed distances between the generated and ground-truth point clouds. However, for small-scale simulated lunar environments, the NeRF model with basic positional encoding outperforms GaussNeRF. Overall, these results suggest that the best density-based NeRF model for large-scale simulated lunar scenes is GaussNeRF, whereas the best density-based NeRF model for small-scale simulated lunar scenes is NeRF with basic positional encoding. Further exploration and optimization is necessary to fully leverage the advantages of GaussNeRF across various lunar scene scales.

Neural Distance Functions

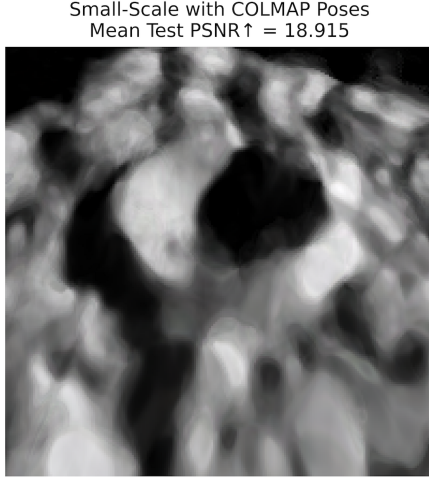


Figure 10: Novel view synthesis results for Experiment 9. GaussNeRF was tested with the small-scale lunar dataset with estimated cameras poses from COLMAP.

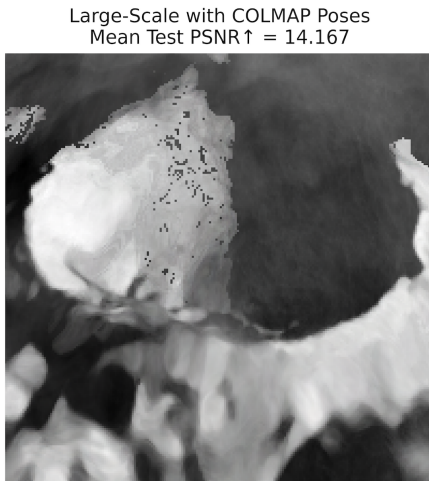


Figure 11: Novel view synthesis results for Experiment 11. GaussNeRF was tested with the large-scale lunar dataset with estimated cameras poses from COLMAP.

Our initial results from NeuS and NeUDF were disappointing, primarily due to inaccurate camera poses and a high learning rate. These issues made it difficult to generate reliable data, especially with NeUDF, where we were unable to produce meaningful output. The high learning rate caused instability during training, and the inaccurate camera poses introduced significant errors in our reconstructions. After addressing these problems, we expect to see substantial improvements. By fine-tuning our camera pose estimation and optimizing the learning rate, expect to achieve more accurate and stable results. The experiments presented here, if anything, highlight how crucial proper hyperparameter tuning and robust data preprocessing are for SDF-based models.

Our improved results with NeuS and NeUDF will be shared in an upcoming publication. For now, our initial novel view-synthesis results from NeuS are presented in *Figure 12*, with the caveat that this figure reflects the early stage of our work and do not fully showcase the method's potential.

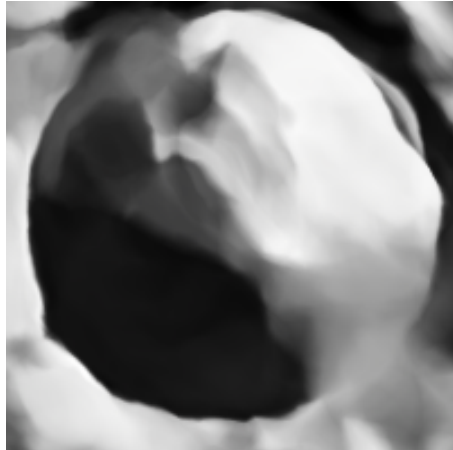


Figure 12: Initial novel view sythesis results with NeuS trained against a large-scale simulated lunar dataset with COLMAP poses and high learning rate.

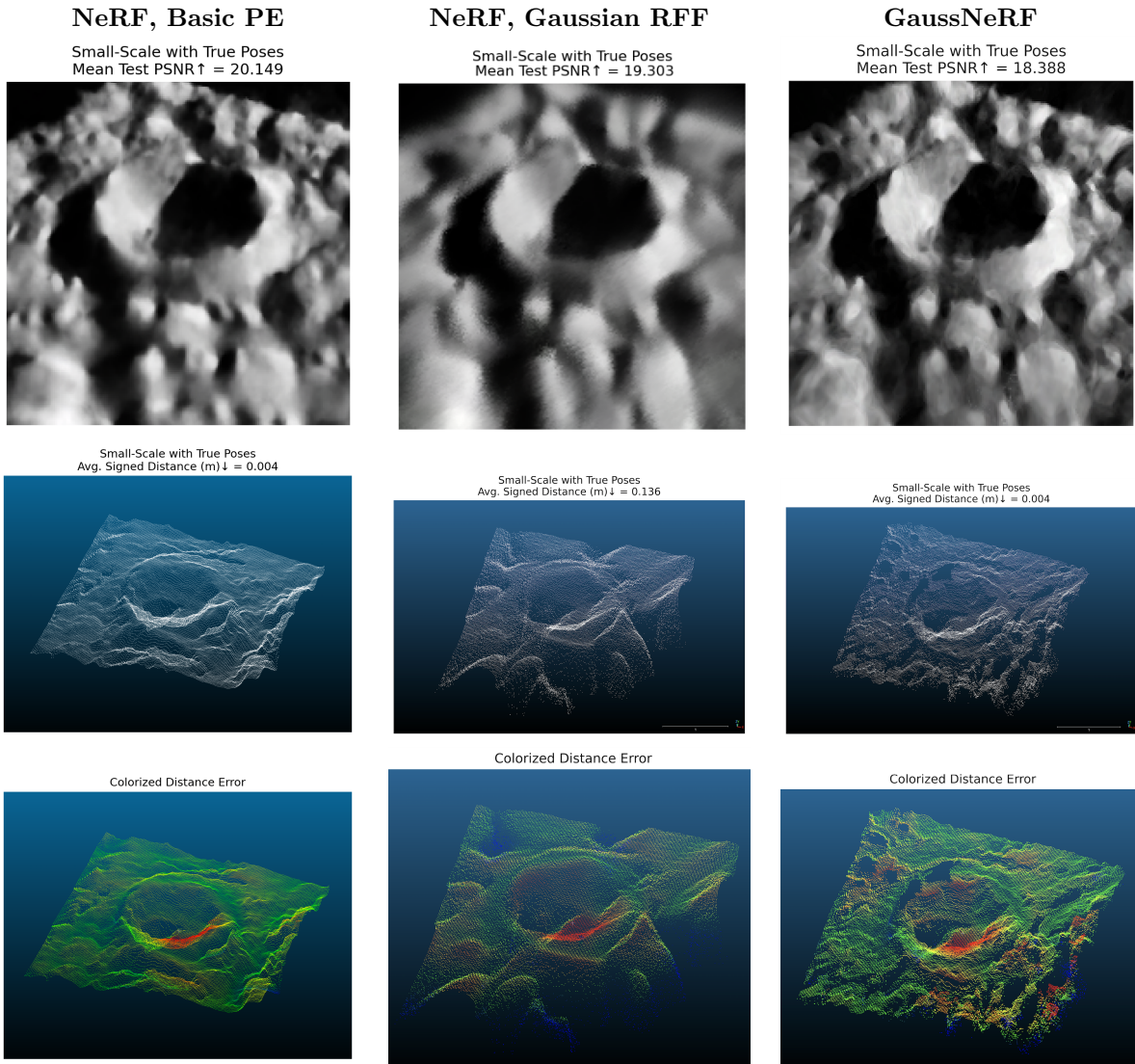


Figure 13: Novel view synthesis (top row), surface reconstruction (middle row), and surface reconstruction colorized by the average signed distance error to the ground-truth (bottom row) for NeRF with basic PE, NeRF with Gaussian RFF PE, and GaussNeRF. The bottom row shows additional results. These methods were tested with the small-scale simulated lunar dataset ($5 \times 5 \times 0.75$ meters) with true camera poses.

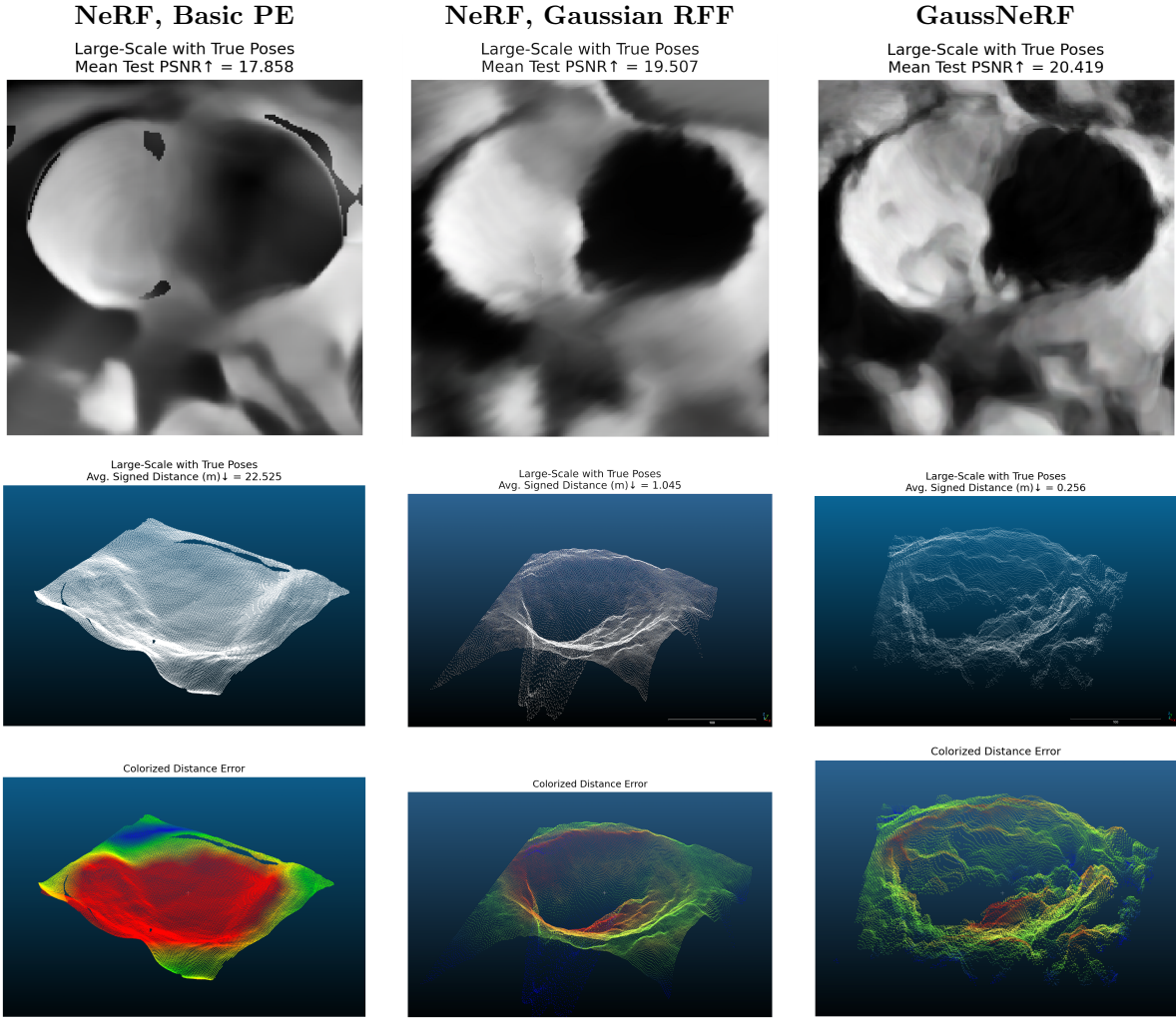


Figure 14: Novel view synthesis (top row), surface reconstruction (middle row), and surface reconstruction colorized by the average signed distance error to the ground-truth (bottom row) for NeRF with basic PE, NeRF with Gaussian RFF PE, and GaussNeRF. The bottom row shows additional results. These methods were tested with the large-scale simulated lunar dataset (700×700×67.4 meters) with true camera poses.

CONCLUSION

This paper has presented initial results from LunarNRM, a neural scene representation method for lunar surface reconstruction, using simulated lunar data. Our initial results show that our LunarNRM method can successfully reconstruct both large-scale and small-scale lunar scenes, making it generalizable to a wide range of lunar surface scenarios. We also show that the use of accurate camera poses improves both novel view synthesis and surface reconstruction

for all models, compared to camera poses estimated with COLMAP.

LunarNRM currently supports both density-based and SDF-based NeRF methods, along with basic and Gaussian RFF encoding. Our initial results suggest that a basic density-based NeRF with a basic positional embedding layer performs best with small-scale lunar imagery with accurate camera poses, achieving a mean PSNR score of 20.149 on test data and a mean signed distance error of 0.0036 meters between the generated and ground-truth point cloud. However, the best density-based NeRF model we tested for reconstructing large-scale lunar scenes was GaussNeRF, which achieved a mean PSNR score of 20.419 on test data and a mean signed distance error of 0.646 meters for the large-scale simulated lunar dataset with accurate camera poses. We are aware of our shortcomings with NeuS and NeUDF, and our more recent findings will be published in the future.

FUTURE WORK

Our future work aims to further enhance LunarNRM to produce physically accurate shadow-free renderings from heterogeneous datasets. One avenue for improvement involves incorporating a wider variety of positional encoding techniques. By exploring and integrating additional encoding methods, we can potentially improve the model’s ability to capture high-frequency details and enhance overall accuracy. We also plan to integrate several other relevant NeRF-based methods into our framework. Specifically, we aim to include a Depth Supervised NeRF (DS-NeRF)¹⁹ and EO-NeRF,⁷ among others. These additions will allow us to more easily experiment with and leverage their unique strengths and innovations, thereby enriching the capabilities of LunarNRM. Another key goal is to add depth supervision and ensure compatibility with processed imagery from the Lunar Reconnaissance Orbiter (LRO). By incorporating depth information and LRO data, we expect to significantly improve the geometric accuracy and reliability of our reconstructions. Lastly, we intend to synthesize our findings from various methods into a more refined and optimized model. This iterative blending of insights and techniques will help us create a more robust and precise solution for lunar surface modeling and relighting, ultimately advancing the state-of-the-art in lunar photogrammetry.

Acknowledgments

We acknowledge that the core contributions used in this paper are NeRFStudio, S-NeRF, and GARF, and we recognize the important contribution of said authors. We hope to build on their work in the future. Our team thanks the NASA Ames Office of the Center Chief Technologist (OCCT) for providing seed funding to begin research into the applicability of NeRFs for space applications.

REFERENCES

- [1] T. Toutin. Elevation modelling from satellite visible and infrared (vir) data. *International Journal of Remote Sensing*, 22:1097–1125, 04 2001.
- [2] High-resolution topography for understanding earth surface processes: Opportunities and challenges. *Geomorphology*, 216:295–312, 07 2014.
- [3] B. Triggs, Philip McLauchlan, R. Hartley, and Andrew Fitzgibbon. Bundle adjustment - a modern synthesis. *ICCV '99 Proceedings of the International Workshop on Vision Algorithms: Theory and Practice*, pages 198–372, 01 2000.
- [4] Ben Mildenhall, Pratul P. Srinivasan, Matthew Tancik, Jonathan T. Barron, Ravi Ramamoorthi, and Ren Ng. Nerf: Representing scenes as neural radiance fields for view synthesis. *CoRR*, abs/2003.08934, 2020.
- [5] Dawa Derksen and Dario Izzo. Shadow neural radiance fields for multi-view satellite photogrammetry. In *Proceedings of the IEEE/CVF Conference on Computer Vision and Pattern Recognition*, pages 1152–1161, 2021.
- [6] Roger Marí, Gabriele Facciolo, and Thibaud Ehret. Sat-nerf: Learning multi-view satellite photogrammetry with transient objects and shadow modeling using rpc cameras, 2022.
- [7] Roger Marí, Gabriele Facciolo, and Thibaud Ehret. Multi-date earth observation nerf: The detail is in the shadows. In *2023 IEEE/CVF Conference on Computer Vision and Pattern Recognition Workshops (CVPRW)*, pages 2035–2045, 2023.
- [8] Peng Wang, Lingjie Liu, Yuan Liu, Christian Theobalt, Taku Komura, and Wenping Wang. Neus: Learning neural implicit surfaces by volume rendering for multi-view reconstruction, 2023.
- [9] Julian Chibane, Aymen Mir, and Gerard Pons-Moll. Neural unsigned distance fields for implicit function learning, 2020.
- [10] Shin-Fang Chng, Sameera Ramasinghe, Jamie Sherrah, and Simon Lucey. Garf: Gaussian activated radiance fields for high fidelity reconstruction and pose estimation, 2022.
- [11] Johannes Lutz Schönberger and Jan-Michael Frahm. Structure-from-motion revisited. In *Conference on Computer Vision and Pattern Recognition (CVPR)*, 2016.
- [12] Johannes Lutz Schönberger, Enliang Zheng, Marc Pollefeys, and Jan-Michael Frahm. Pixel-wise view selection for unstructured multi-view stereo. In *European Conference on Computer Vision (ECCV)*, 2016.
- [13] Sebastian Bullinger, Christoph Bodensteiner, and Michael Arens. A photogrammetry-based framework to facilitate image-based modeling and automatic camera tracking, 2021.
- [14] Nerfacto. <https://docs.nerf.studio/en/latest/nerfology/methods/nerfacto.html>.
- [15] Ellemieke Van Kints Aiden Hammond Caleb Adams, Ignacio Lopez-Francos. A summary of neural radiance fields for shadow removal and relighting of satellite imagery, 2023.
- [16] Splatfacto. <https://docs.nerf.studio/nerfology/methods/splat.html>.
- [17] Ben Mildenhall, Pratul P Srinivasan, Matthew Tancik, Jonathan T Barron, Ravi Ramamoorthi, and Ren Ng. Nerf: Representing scenes as neural radiance fields for view synthesis. *Communications of the ACM*, 65(1):99–106, 2021.
- [18] Matthew Tancik, Pratul P. Srinivasan, Ben Mildenhall, Sara Fridovich-Keil, Nithin Raghavan, Utkarsh Singhal, Ravi Ramamoorthi, Jonathan T. Barron, and Ren Ng. Fourier features let networks learn high frequency functions in low dimensional domains, 2020.
- [19] Kangle Deng, Andrew Liu, Jun-Yan Zhu, and Deva Ramanan. Depth-supervised nerf: Fewer views and faster training for free, 2022.